INVESTIGATIONS OF ELECTRON EMISSION CHARACTERISTICS OF LOW WORK FUNCTION SURFACES

Report No. 2

By

L. W. Swanson
A. E. Bell
L.C. Crouser
B.E. Evans

Prepared for

Headquarters
National Aeronautics and Space Administration
Washington, D. C.

Quarterly Report No. 2
28 December to 27 March 1967

April 1967

CONTRACT NAS w-1516

FIELD EMISSION CORPORATION
Melrose Avenue at Linke Street
McMinnville, Oregon 97128

TABLE OF CONTENTS

LIST OF ILLUSTRATIONS

PURPOSE

The primary purpose of this work is to gain an improved fundamental understanding of

(1) the phenomena governing the production of low work function surfaces, and

(2) the factors affecting the quality and stability of electron emission characteristics.

It is anticipated that information generated from this investigation will be relevant to various kinds of electron emission (i.e. , photo, thermionic and field emission), although the primary emphasis is placed upon field emission.

The formation of low work function surfaces is accomplished by:

(1) adsorption of appropriate electropositive adsorbates, and

(2) coadsorption of appropriate electropositive and electronegative adsorbates.

Various properties of these surfaces investigated in order to obtain a more fundamental understanding of them are the temperature dependency of the emission and work function, the various types of energy exchanges accompanying emission, the energy distribution of the field emitted electron, and various aspects of the surface kinetics of adsorbed layers such as binding energy, surface mobility and effect of external fields.

ABSTRACT

This report describes thermal and field desorption of *Cs* from a fluorinated tungsten surface. The binding of *Cs* to a W substrate is increased by the presence of coadsorbed F. The field desorption of Cs from a FW surface occurs at low temperatures without disturbing the underlying FW layer.

The time stability of the field emission current from a clean or Zr/O coated tungsten surface is greatly enhanced if positive ions formed at the electron collector surface are not allowed to return to the emitter cathode.

INTRODUCTION

Work has continued this quarter on the desorption characteristics of the CsFW system. The following behavior for cesium and fluorine adsorption on tungsten have been found from earlier work.[1,2] Adsorption of cesium on fluorine-covered tungsten results in work function minima as low as 1.0 eV which are thermally stable to 500°K. The migration activation energy of Cs on FW was found to increase with underlying F coverage. The adsorption of CsF was found to be dissociative, and differential migration of Cs and F was observed. At low work functions, near the minima, high negative fields applied to the tip gave rise to I changes explainable only by field desorption of F^-. A FW layer was found to be stable to 1400°K; however, a small amount of Cs enhanced the removal of F at temperatures above 875°K, presumably by thermal desorption of CsF. The initial F from a CsFW surface could be retained on a tip heated above 875°K by applying a positive field of 2, 4 MV/cm to the tip.

In this quarter, studies have been made of the effects of a F layer on the desorption temperature of Cs and the field desorption of cesium from an F-covered surface.

EXPERIMENTAL

The field emission microscope used has separate sources for Cs and CsF addition and has been fully described in previous reports.[1,2] Average work function changes were determined from the total emission current I and the applied voltage V analyzed by the well-known Fowler-Nordheim equation;

$$I = AV^2 \exp\left[-b\phi^{3/2} v(y)/\beta V\right], \qquad (1)$$

where A is the pre-exponential constant, ϕ the average work function, β the geometric factor relating $\beta = F/V$ and the image c'orrection v(y) is an almost

linear function of $y = 14.4\ F/@^2$ with energies in eV and lengths in Å. The value of ϕ for an adsorbate-covered emitter can be obtained relative to the clean value ϕ_s, assumed to be 4.52 for W, by comparing the clean and adsorbate-coated slopes m_s and m of a Fowler-Nordheim plot of $\ln I/V^2$ vs I/V, from whence

$$\phi = \phi_s (m/m_s)^{2/3} \qquad (2)$$

Implicit in the utilization of Equation (2) is the constancy of β upon adsorption.

Thermal Desorption. - CsF was deposited on the tip at 77°K. A positive field of 2.4×10^6 V/cm was applied to the tip and the tip was heated to 1200°K. This procedure was repeated until the desired F coverage was attained as indicated by the work function.

Cs was then adsorbed in uniform doses to a monolayer. The tip was then heated in steps to 1900°K with 60 seconds per step at temperatures below 1200°K and 10 seconds per step above 1200°K. The tip was cooled to 77°K between each step, and the work function measured. A positive 2.4×10^6 V/cm field was applied during each heating so that the initial F would be retained. This also allows Cs to be removed in ionic form when $\phi > 3.87$ eV. From these observations, together with adsorption curves, the desorption temperature versus coverage curves were obtained for three underlying fluorine coverages. The results are shown in Figures 1 and 2. The terminal coverage desorption temperature of Cs^+ is found to increase as the F coverage increases.

Field Desorption. - CsF was deposited on clean tungsten and the Cs removed, leaving only a F layer with a $\phi = 5.08$ eV. A positive field was applied to the tip and increased stepwise until the Cs was removed, leaving only a bright ring around the edge of the screen. At high Cs coverages, the field desorption process is regenerative and the whole tip is rapidly cleaned to the outer edges. This is because the field required for desorption drops

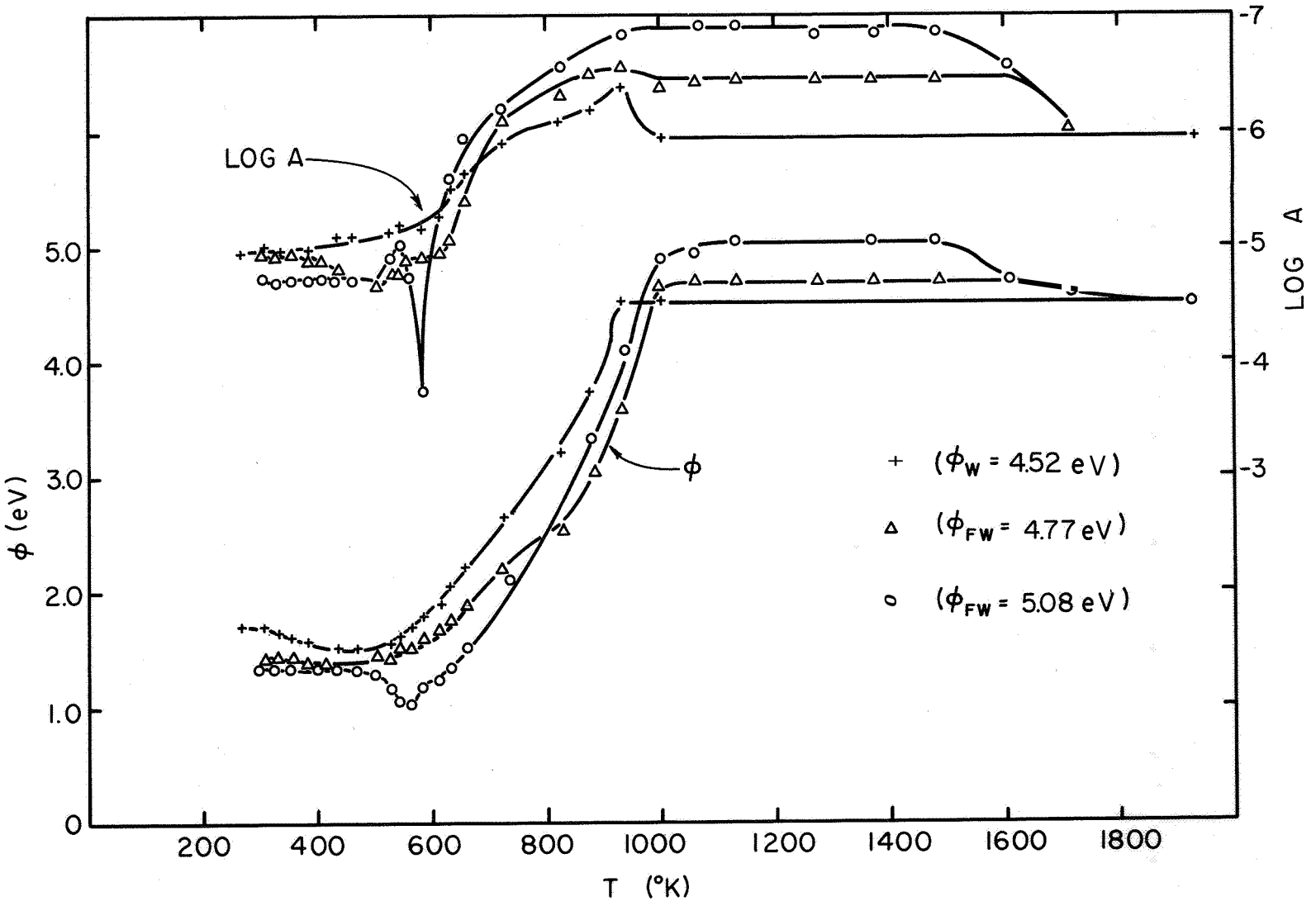

Figure 1. Curves show the variation of ϕ and $\ln A$ upon heating a fully cesium coated FW surface at the indicated temperatures for 60 sec intervals. During heating the screen was biased to -185 V (F = 2.0 MV/cm).

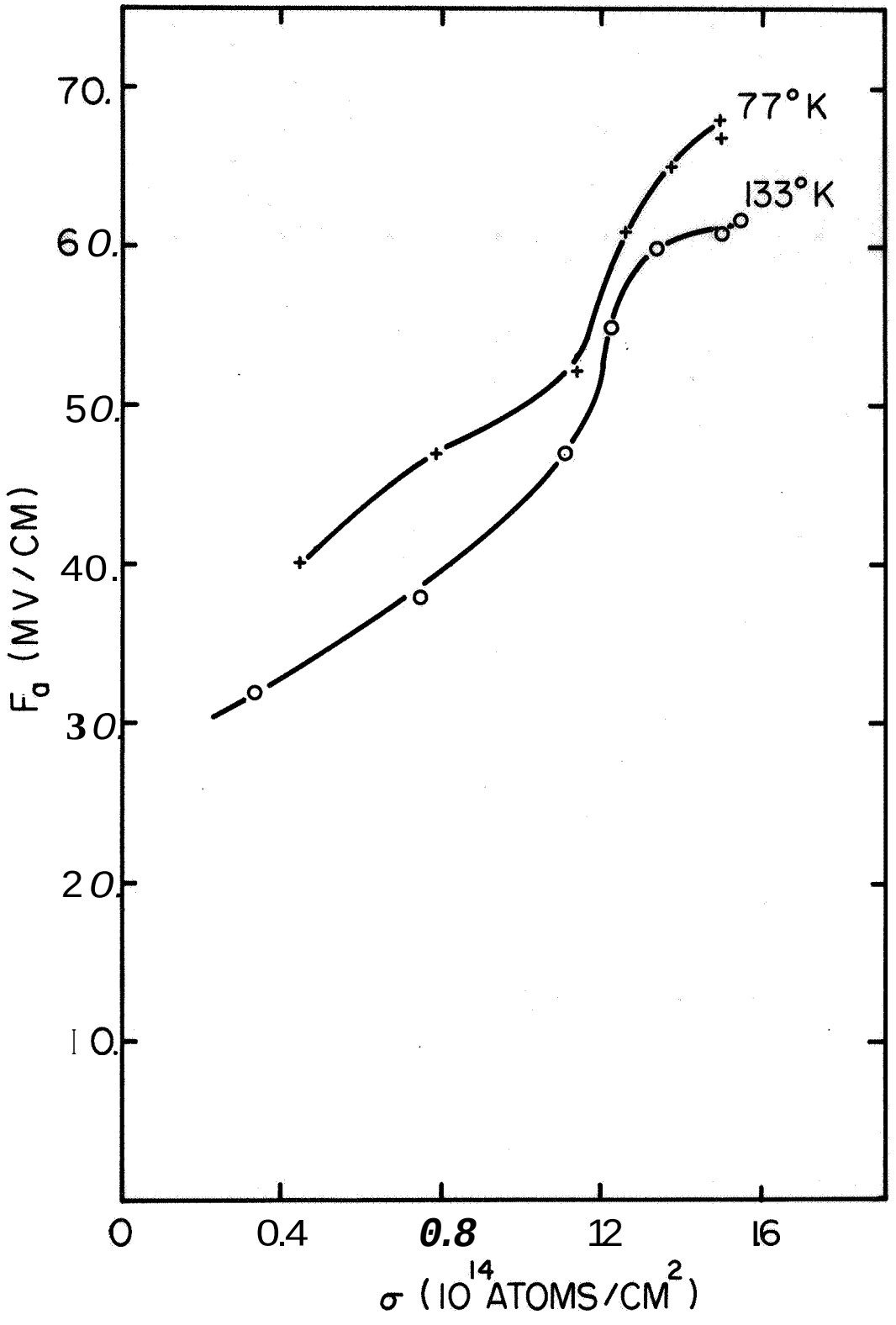

Figure 2. **Curves show the positive field required to initiate desorption of Cs as a function of Cs coverage from an FW surface where $\phi_{FW} = 5.09$ eV.**

sharply with coverage in the high coverage region and the process, once initiated, goes rapidly to completion. At lower coverages, the field desorption is slower and the process is observable. Figure 3 shows a sequence of patterns as the desorption field is increased, starting with a Cs coverage of (0.5×10^{14} at/cm^2). The F is seen to remain behind as can be seen from the F pattern (f) of Figure 3.

DISCUSSION

Thermal Desorption

The relation between the activation energy for neutral desorption E_a and ionic desorption E_P is

$$E_p = E_a + I - \phi \qquad (3)$$

where I is the ionization potential of the adsorbate (3.87 V for Cs) and ϕ the work function. Thus if the surface is biased positively, desorption in ionic form becomes more economical (i.e., $E_P < E_a$) when $\phi > 3.87$ eV. Since for terminal coverage desorption in the Figure 1 results $\phi > 3.87$ eV, desorption of Cs occurs primarily in ionic form. In view of the fact that the terminal coverage work function ϕ_{FW} increases from 4.52 to 5.08 eV, one expects a reduction in E_P if E_a is constant. Figure 1, however, shows an increase in the desorption temperature T_P, where $T_P \cong E_P/k$, with increasing ϕ_{FW}. We therefore conclude that the underlying chemisorbed F layer increases E_a at least 0.6 eV at the maximum F coverage.

Upon desorption of the Cs, subsequent desorption of F begins at 1500°K and is completed at 1800°K according to the Figure 1 results.

Field Desorption

In previously reported work field desorption of F^- has been verified at low values of work function for the CsFW system. In this section we

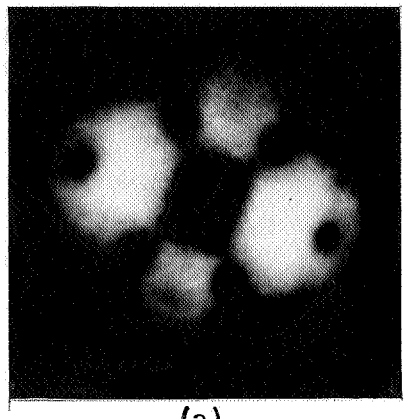

(a)
Clean W

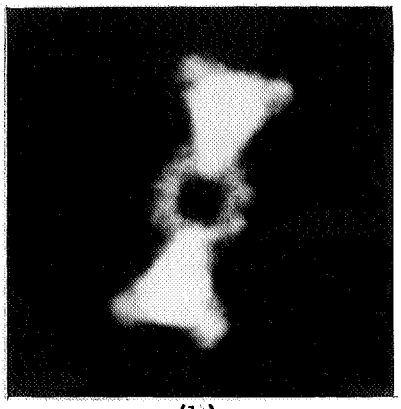

(b)
Initial fluorine deposit;
ϕ_{FW} = 4.81 eV

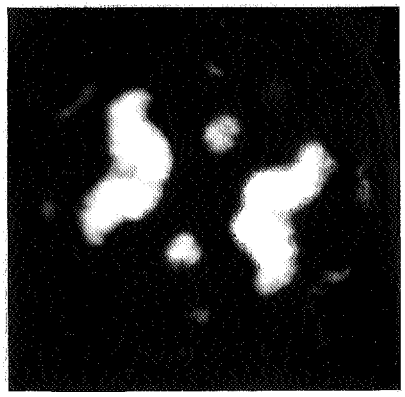

(c)
Initial CsFW layer;
ϕ_{CsFW} = 3.58 eV

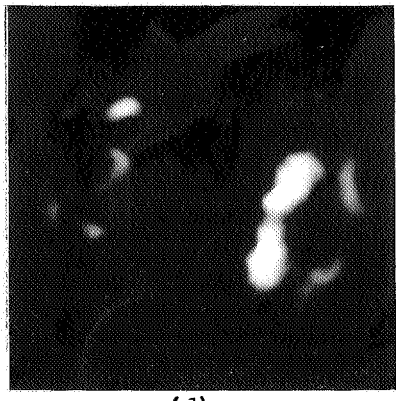

(d)
Field desorption at
F = 41.4 MV/cm

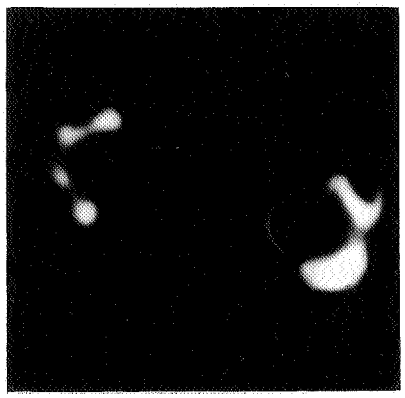

(e)
Field desorption at
F = 46.5 MV/cm

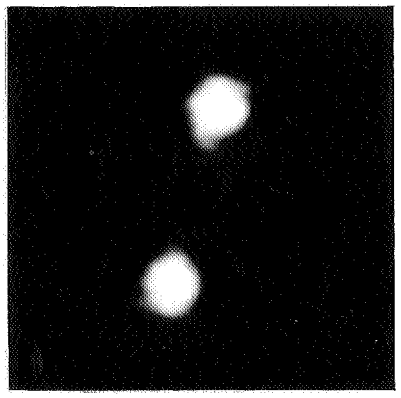

(f)
Field desorption at
F = 56.8 MV/cm;
$\phi \cong$ 4.8 eV.

Figure 3. Pattern sequence showing progress of field desorption at 77°K. Note pattern **(f)** is very similar to (b) indicating removal of Cs from the F W surface.

discuss the field desorption of Cs^+ in positive applied fields. To include the effect of applied field F_a Equation (3) becomes modified

$$E_p = E_a + I - \phi - e^{3/2} F_a^{1/2} + aF_a + bF_a^2 \qquad (4)$$

the terms linear and quadratic in F_a include field induced work function and polarization corrections which are normally small compared to the $F_a^{1/2}$ term. Equation (4) predicts E_P to decrease with increasing ϕ; since ϕ increases $\sim$4.0 eV while E_a increases only $\sim$ 2 eV with decreasing coverage of Cs, E_P decreases with σ and the field desorption of Cs is regenerative for $\sigma < \sigma_m$. This regenerative feature has been observed both for clean and fluorinated substrates.

In Figure 2 the values of F_a required to initiate field desorption of Cs^+ from a CsFW layer are plotted as a function of Cs coverage. In the temperature range investigated, desorption occurs between 30 and 70 MV/cm. The increase in F_a with Cs coverage stems primarily from the decrease in ϕ.

That Cs is desorbed leaving an undisturbed FW layer is established from the sequence of patterns in Figure 3, where the original FW pattern (photo f) reappears after field desorption of the Cs. The removal of Cs begins near the emitter apex due to the higher electric field, then proceeds outward toward the periphery of the emitter. It can be concluded that field desorption does not remove CsF, but rather favors rupture of the CsF bond.

CATHODE LIFE STUDIES

Introduction

Initiation of a cathode life study of zirconium and oxygen coadsorbed on tungsten field emission cathodes was begun last quarter.[2] This study was initiated in order to gain insight into the life and stability of low work function coated tungsten field emission cathodes. The main interest lay in the determination of mechanisms involved in cathode current deterioration

durihg operation and the possibility of increasing the stability and life of such a cathode by minimizing effects contributing to coating deterioration.

There are two physical processes by which field emitted current from a clean surface may vary with time. One is geometric change in the emitter surface caused by bombardment of high energy positive ions formed in the gas phase or at the anode surface. The other process involves work function change due to adsorption of neutral gas molecules on the emitter surface. Since ionic bombardment roughens the surface, microscopic protrusions are usually formed which enhance the local electric field and, hence, current. Gas adsorption, on the other hand, nearly always increases the work function, thereby decreasing the field emission current. In the case of an adsorbate coated emitter which lowers the work function, ionic bombardment may not only roughen the surface, but also sputter the low work function adsorbate, thus leading to a current decrease with time.

In view of the fact that field emission current instability occurs even in high vacuum field emission tubes and is generally proportional to the emitted current, it appears plausible that both ionic and neutral bombardment of the emitter is caused by the now well-known process of electron induced desorption of ions and neutrals from the anode surfaces. The specific purpose of the study is to examine the origin of these ions by attempting to suppress ionic bombardment of the emitter by creating potentia1 saddles for ions in front of the emitter surface and by reducing the collected electron energy below the threshold for electron induced desorption.

Experimental

A new tube was designed and constructed which more effectively utilized an axial magnetic field for confining the electron beam. A schematic diagram of the tube employed in this experiment is shown in Figure 4 and is quite similar in design to the tube used previously.[2] The basic difference is in the envelope design which permits the tube to be immersed in the magnetic field of a horseshoe-type magnet. Another change to achieve more

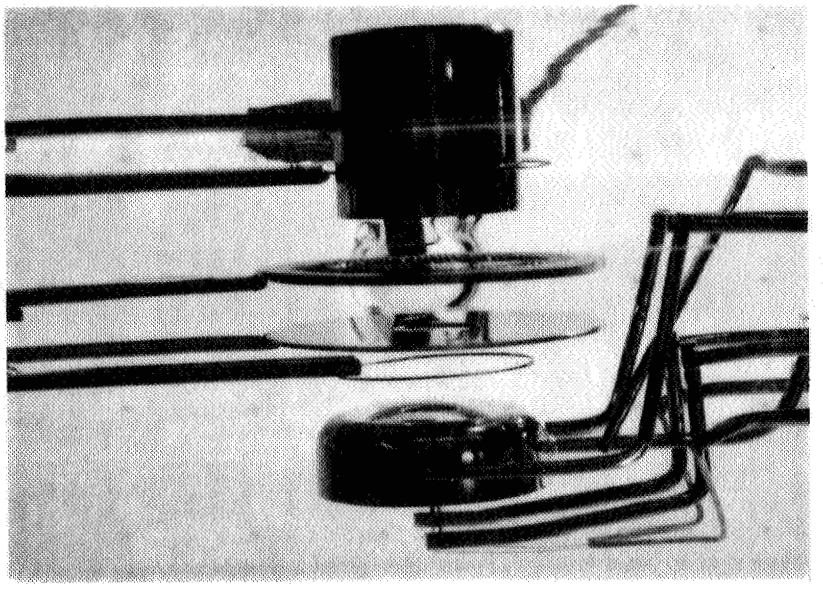

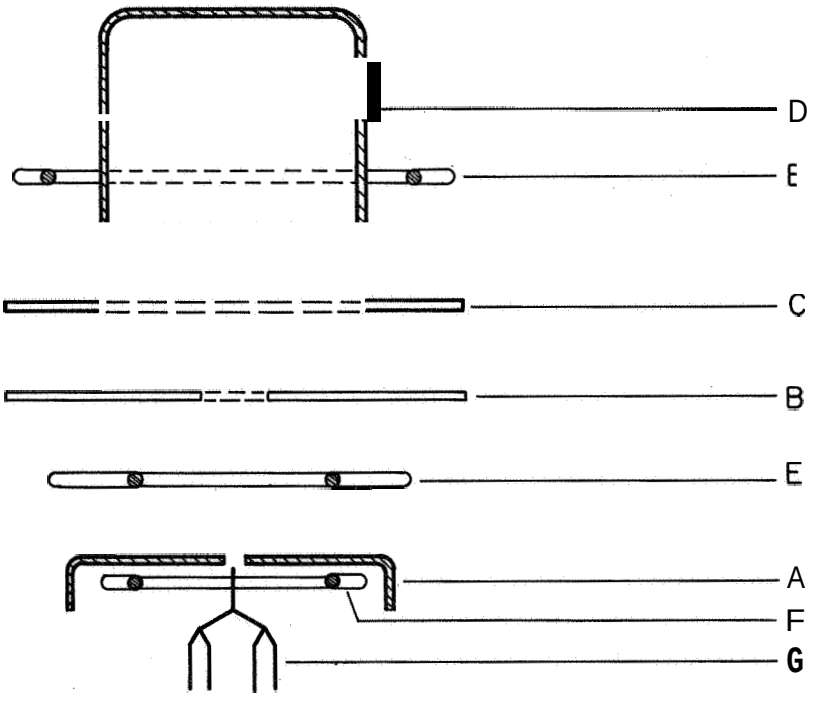

Figure 4. Schematic diagram and photograph internal components of life test tube showing; A - first electrode, B- second electrode, C - screen grid, D - Faraday cup, E - outgasing filaments, F - zirconium source, and G - cathode.

effective shielding of the cathode with respect to ions formed at the collector electrode was construction of electrode **A** from a 5/8 inch diameter molybdenum cup with a 150 mil aperture in the center for passage of the electron beam. This design was expected to yield good collection of the electron beam in the Faraday cage D at electron energies below electron impact desorption values and essentially eliminate ion and neutral production by electron impact. It was found however, that the screen grid C, placed in front of the Faraday cage to suppress secondaries and reflected electrons, was a source of secondary or reflected electrons itself. Even though the suppressor screen was highly transparent, it was found nearly impossible to prevent the secondary electrons formed at the screen from returning to electrode **A** (which was the anode) where they were collected at high energy. This effect occurred even though the electrode B was held at cathode potenital and seemed to be the result of field lines from the electrode **A** bulging through the aperture of electrode B, thereby causing electrons from the screen to be accelerated back to electrode **A.**

Experimental Results

In order to achieve good collection of the primary beam current I_t in the Faraday cage ($\geq 99\%$ of the emitted electrons) it was necessary to operate the Faraday cage at voltages of the order of the electrode **A,** In so doing, it was found that secondaries created at the screen grid were then attracted to the positive Faraday cage. Collection of electrons at the higher energies resulted in electron impact desorption of ions and neutrals at the cage and acceleration of these ions back toward the cathode. However, since the first electrode was normally the highest positive element in the tube, a positive potential hump was formed and thus served as a barrier for ions created on all but the first electrode from returning to the cathode G. By operating the tube in this manner, it was possible to achieve excellent collection at the Faraday cage, suppress ions from bombarding the cathode and prevent both secondaries from returning to the electrode **A** where more ions might be created. Table I gives the operating voltages and the current ratios measured at the various elements of the tube shown in Figure **4,**

Operation of the tube in the mode described above was carried out for a Zr/O coated and clean tungsten cathode and was compared with operation of the tube in a simple diode configuration. Figure 5 shows the results of operation in the two modes for both clean and coated tungsten cathodes.

TABLE I

Electrode Potentials and Current Ratios for Figure 5 Data

Run	V_A(kV)	V_B(Volts)	V_C(Volts)	V_D(kV)	I_D/I_t	I_A/I_t
A	3.9	490	98	3.8	.99	.01
B	6.4	0	99	6.3	.99	.01
C	3.8	3.8	3.8	3.8	---	---
D	6.1	6.1	6.1	6.1	---	---

Conclusion

The effect of ion bombardment on both clean and Zr/O coated tungsten field emission cathodes is quite apparent from the Figure 5 results. Operation of the tube in the ion and secondary suppression mode shows marked improvement in cathode performance in both cases. The fact that ion bombardment of the cathode causes the current from the Zr/O coated cathode to decrease and from the clean tungsten cathode to increase with time is a demonstration of the different effects of ion bombardment on the two surfaces. A deterioration of the coating leads to an increase in the work function toward that of the clean substrate. On the other hand, ion bombardment of the clean surface results primarily in a roughening of the surface, which in turn leads to field enhancement and a resulting rise in current.

Elimination of ions from striking the cathode greatly improves the stability for both cases. For the Zr/O surface, a rapid drop during diode operation is changed to a slow increase in current when the cathode is operated in the ion suppression mode. The same behavior is observed in the

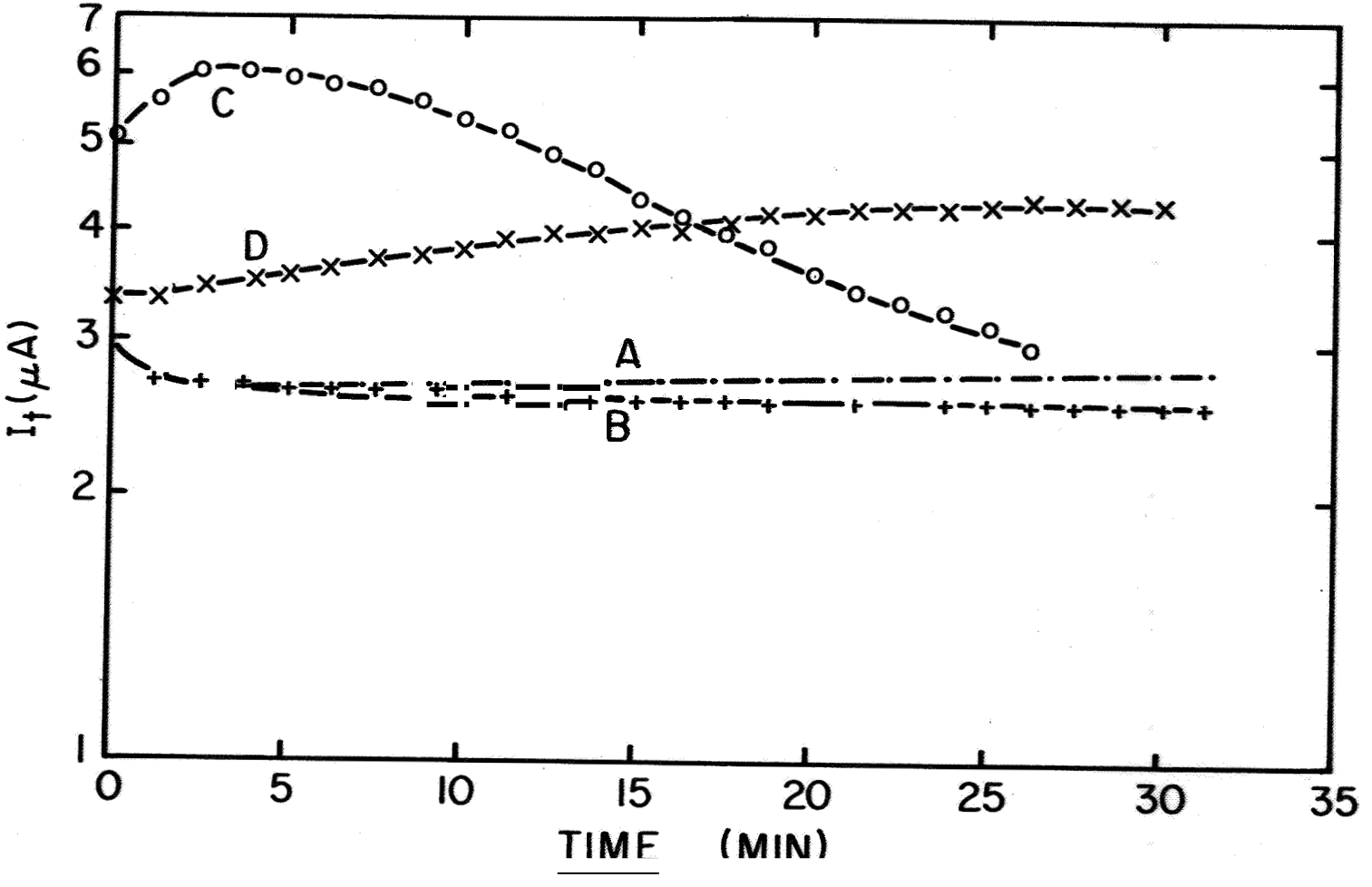

Figure 5. Stability tests taken with and without ion and secondary trapping for both clean (B, D) and zirconium coated (A, C) tungsten. Electrode operating parameters given in Table I.

clean tungsten case, only the effects are reversed; a fairly rapid increase in current during diode operation is changed to a slow decrease in current during ion suppression operation. Since collection of the electrons at the collector surface was well above the threshold for electron induced desorption of ions and neutrals, it is probable that the small changes in current with time observed during the ion suppression mode of operation was caused by neutral species desorbed from the collector surface which readsorbed on the emitter during operation. In conclusion, it is clear that ion impact of the cathode surface is the primary cause of current instability and a definite improvement in cathode life is the result of reducing or eliminating ion bombardment of the cathode during operation.

ENERGY DISTRIBUTION STUDIES.

Previous work on the total energy distribution of field emitted electrons from various planes of tungsten has shown that certain results, from single crystal planes are not predicted by the field electron model, and anomalies in the energy distribution from the (100) and (110) planes of tungsten have been detected. It now seems fruitful to investigate the energy distribution from other refractory metals in order to compare them with the tungsten results. A particularly good choice would be molybdenum since its electronic band structure is now relatively well-known and its geometric structure is identical to that of tungsten. It would also be informative to study the effect of adsorption on the energy distribution, particularly in view of recent papers which suggest definite effects on the energy distribution depending on the bonding mode of the adsorbate.

A study along these lines has been initiated with the construction of a new energy distribution tube. This tube is of the same design used previously,[1] but the zirconium source has been replaced by a cesium zeolite source consisting of a sodium aluminosilicate molecular sieve powder (Linde type A zeolite) which has undergone an ion exchange reaction with cesium as described by Weber and Cordes.[3,4] The material was then

coated onto a platinum filament and, upon heating to 1100°K, could be used as a very effective source of cesium with impurity content less than 0. 5%.

A molybdenum emitter has been sealed into the energy distribution tube and results are currently being obtained.

FUTURE WORK

During the coming quarter results of the energy distribution of field emitted electrons from clean and cesium-coated molybdenum will be obtained. A probe field emission study of the CsOW system will be initiated. Also, a field emission investigation of the HgW and HgOW systems will be undertaken.

REFERENCES

1. L, W. Swanson, et al. , Final Report, Contract NAS w-1082, Field Emission Corporation, Sept. 1966.
2. L. W. Swanson, et al. , Report No. 1, Contract NAS w-1516, Field Emission Corporation, Feb. 1967.
3. R. E. Weber and L. F. Cordes, Report on 25th Annual Conference on Physical Electronics 378 (1965).
4. R. E. Weber and L. F. Cordes, Rev. Sci. Instr. 37, 112 (1966).

QUARTERLY **DIS**TRIBUTION LIST

Contraet NASw 1516

NASA Headquarters	
Washington, D. C. 20546	
Attn: Dr. R. R. Nash - Code RRM	4
G, Pfannebecker - Code RNT	1
T. Tsacoumis - Code REG	1
Scientific and Technical Information Facility	
Attn: NASA Representative	
Post Office Box 5700	
Bethesda, Maryland 20014	2
NASA Lewis Research Center	
Cleveland, Ohio 44135	
Attn: Dr. R. Breitweiser, Section 2131	1
Dr. R. A. Lad, Section 2330	1
J, Ferrante, Section 9711	1
D. L. Lockwood, Section 9711	1
Dr, H. Schwartz, Section 9213	1
Dr. L. Tower, Section 2132	1
NASA Marshal1 Space Flight Center	
Huntsville, Alabama	
Attn: Dr. I. Dalins, Code R-RP-N	1
NASA Electronic Research Center	
Cambridge, Massachusetts	
Attn: Dr. M. S. Macrakis, Code CT	1
U.S. Naval Ordnance Test Station	
Physics Division, Michaelson Laboratory	
China Lake, California 93556	
Attn: Dr. E. Bower, Head	
Crystal Physics Branch	1
National Bureau of Standards	
Atomic Physics Division	
Washington, D. C. 20546	
Attn: Dr. R. D. Young	
Electron Physics Section	1

Professor Robert Gomer
Institute for the Study of Metals
University of Chicago
Chicago, Illinois 60637 1

Professor W. L. Boeck
Department of Physics
Niagara University
Niagara University, New York 14109 1